Mars Science Laboratory's Dust Removal Tool

Kiel Davis*, Jason Herman*, Mike Maksymuk*, Jack Wilson*, Philip Chu*[1],
Kevin Burke**, Louise Jandura** and Kyle Brown**

Abstract

The Dust Removal Tool (DRT) is designed to expose the natural surfaces of Martian rocks obscured by layers of dust deposited by aeolian processes. The DRT, contained within a cylinder 154-mm long and 102-mm in diameter, has a mass of 925 grams. Using a single brushless DC motor, the DRT removes dust from an area 45 mm in diameter. During the dust removal process, a set of brushes articulate to maintain surface contact as they rotate at high speed. The DRT belongs to a special class of aerospace mechanisms designed to interact with unstructured extraterrestrial surface objects and environments. The wide range of rock surface characteristics along with severe resource constraints makes the DRT solution non-trivial. The mechanism features a high reduction single-stage planetary gear box and pivoting brushes that both offered lessons learned. The flight unit DRT was integrated with the MSL rover in early 2011 and is currently on track to begin surface operations at Mars' Gale Crater in August 2012.

Introduction

The Dust Removal Tool (DRT) is a critical component of Mars Science Laboratory's (MSL) Sample Acquisition, Sample Processing and Handling (SA/SPaH) subsystem. The aeolian-deposited reddish iron oxide dust that covers everything on the surface of Mars masks many characteristics of rocks and makes it difficult for scientists to identify optimal rock targets for further interrogation and possible sample acquisition. For instance, as shown in Figure 1, dust layers only microns deep can obscure many visual clues to a rock's origin (e.g., color or emissivity, cracks and inclusions) from instruments like the MSL's MastCam and Mars Hand Lens Imager [1]. MSL's Alpha-particle X-ray spectrometer (APXS), a key source of information about a rock's elemental composition, is effectively blinded by layers of dust as little as 5 microns deep [2]. It is therefore critically important to remove dust from the surface of rocks.

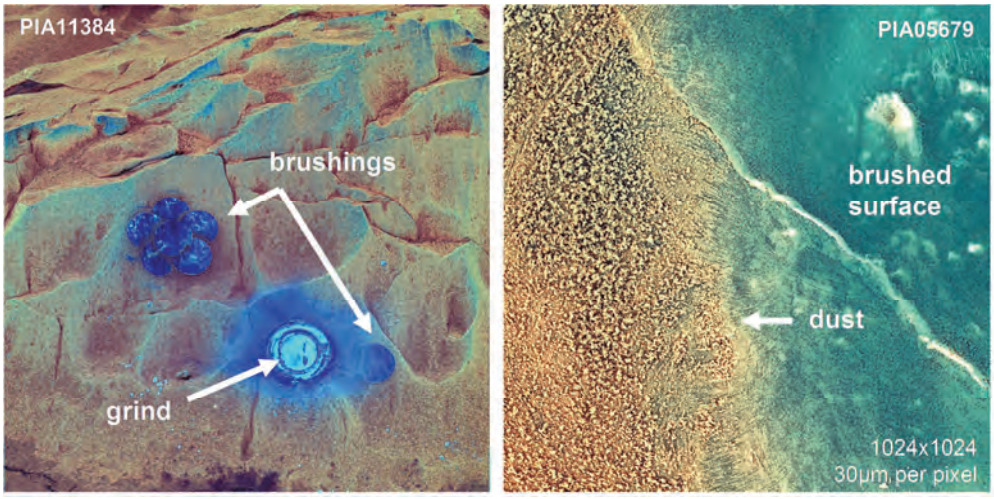

Figure 1. Left: MER Spirit Pancam false-color image of Mazatzal on Sol 86 after numerous Rock Abrasion Tool brushing and grinding operations; Right: MER Spirit Microscopic Imager false-color image of Mazatzal on Sol 79 after a RAT brushing operation. Image credit: NASA/JPL-Caltech/Cornell

* Honeybee Robotics Spacecraft Mechanisms Corp., New York, NY
** Jet Propulsion Laboratory, California Institute of Technology, Pasadena, CA

Planetary scientists may have first appreciated the dust's complicating effect during the Mars Pathfinder mission where APXS data were contaminated by dust and meaningful inferences could only be drawn through a process that assumed an amount of dust that had to be subtracted from the spectra [1]. Unlike Mars Pathfinder, the Mars Exploration Mission rovers Spirit and Opportunity both carried a tool for doing away with the dust a rock's surface. This tool, developed by Honeybee Robotics, is called the Rock Abrasion Tool (RAT) [4]. The RAT's primary purpose is to remove the rock's weathered rind by grinding an area 45 mm in diameter to a depth of 5 mm. By accomplishing its primary objective it naturally has to also remove surface dust. The RAT is equipped with brushes for sweeping away cuttings produced during the grinding process – see Figure 2. During the initial stages of RAT development, it was never envisioned or required that the RAT's brushes be used to strictly brush away surface dust layers. But through experimentation before and during the MER mission, it was eventually found that the RAT's high-speed brush, which protruded several millimeters beyond the grinding wheel's reach, is particularly effective at removing even fine layers of dust from all manner of rocks including those with pitted, vesicular surface textures.

The RAT can also accommodate a large degree of surface topography variation and robotic arm (IDD) positioning error due to its design architecture and 3 degrees of freedom. Prior to brushing or grinding, the IDD preloads the RAT against the surface of the rock via the RAT's butterfly mechanism (see Figure 2). The RAT has three actuators including a Z-axis actuator which moves the grinding wheel and brushes linearly toward and away from the rock surface. Once preloaded, a RAT software algorithm employing all three actuators, detects the rock's local surface position in the Z-axis reference frame. The RAT grind brush is then positioned with respect to the surface such that its bristles are engaged and the grinding wheel is not engaged. In this way, the arm positioning error is rendered more or less moot and successful brushing is achieved on a wide range of uneven surfaces.

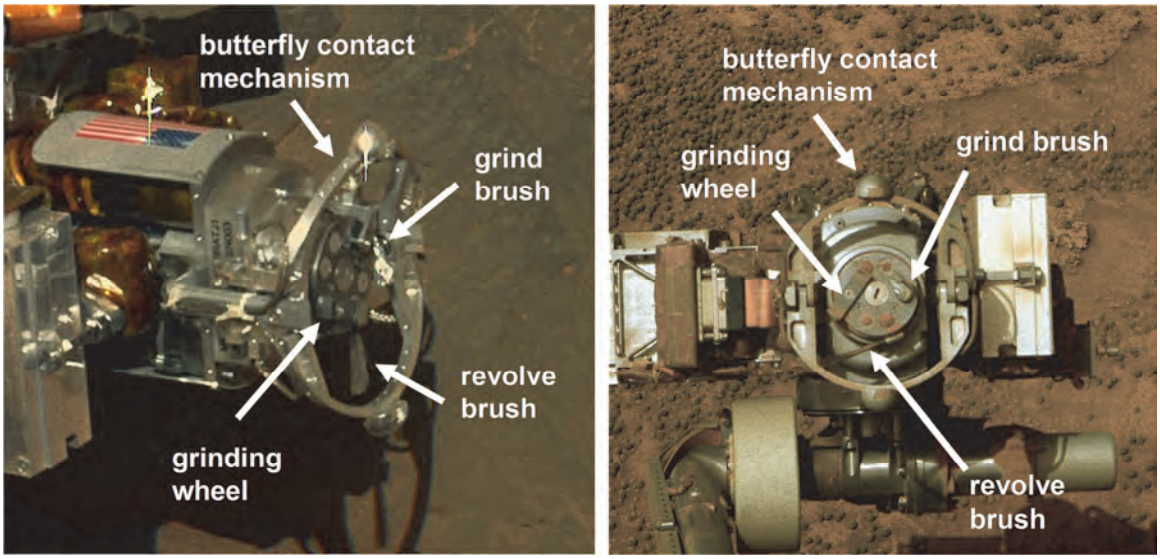

Figure 2. Left: MER Spirit RAT on Mars prior to its first operation on Adirondack rock; Right: MER Opportunity RAT on Mars after many operations. Image credit: NASA/JPL-Caltech/Cornell

The original plan for MSL was to include a next generation RAT with all the same functionality as the MER RAT but designed to last longer and penetrate stronger rocks [5]. However, that tool was eventually descoped by the JPL flight project office in 2007 to meet project budget constraints. This left the MSL science team without a method for clearing the blinding dust from rock surfaces. So later in 2007 a new effort was initiated to develop a tool, the DRT, designed solely for the purposes of removing dust.

Like other MSL mechanisms [6], the DRT is designed for very long life in very harsh conditions. But the DRT is unique and interesting for at least two reasons. First, as a device that directly, physically engages

an extraterrestrial object (rock) so as to manipulate this object's characteristics in some way, the DRT belongs to a special class of aerospace mechanisms. In this context, it is interesting and informative to future missions to understand how the DRT design solves the difficult problem of adequately removing micron-scale particles from a rock's uneven and often pitted surface. Second, from a pure mechanisms perspective, the DRT offers a valuable data point for planetary gear box designers along with other lessons. Due to extreme volume constraints, there was just enough room for a single stage planetary gear reduction necessary for meeting torque margin requirements. Practical limits of planetary stage reductions are considered 3:1 (lowest, planets become very small) to 10:1 (highest, sun becomes very small). A ratio closer to 5:1 is the most balanced with the highest performance rating and is therefore more common in space mechanisms designs. The DRT design incorporated a 10.4:1 single stage planetary gear reduction which pushes the limits of what is conventionally considered practical.

This paper will provide an overview of the DRT including requirements, design, manufacturing and qualification testing. It will present some of the key trades made during the development process including brush articulation kinematics and bristle geometry to maximize the reachable workspace. A significant part of the paper will deal specifically with brush pivot torque margin problems, the planetary gear design and related test results.

DRT Overview

The DRT is mounted on the MSL robotic arm (RA) turret as shown in Figure 3. Once placed on a rock by the RA, the DRT's primary functional requirement is to clear dust layers up to 2 mm deep from an area on the rock's surface no less than 45 mm in diameter – this diameter is driven by the APXS field of view and RA positioning accuracy. Like the MER RAT, the DRT is expected to face all kinds of rocks with diverse surface textures and topographies. Unlike the MER RAT however, the DRT only has a single actuator and is not preloaded against the surface. The design must therefore accommodate robotic arm positioning error in addition to varying local rock surface topography. These new design and operational constraints were challenging and required a substantial departure from the heritage RAT brush design.

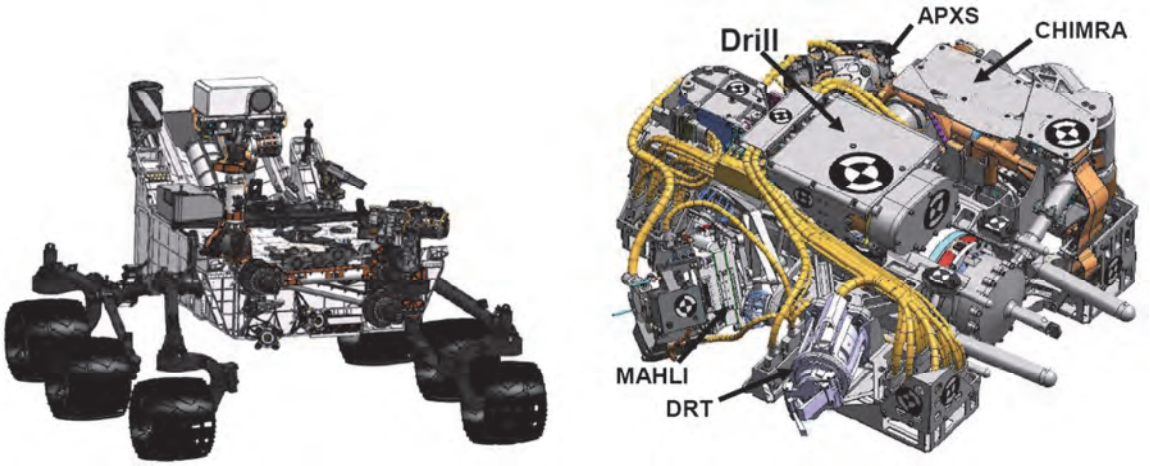

Figure 3. Left: MSL rover; Right: SA/SPaH turret with DRT. Image credit NASA\ JPL-Caltech [6]

To deploy the DRT, the RA first confirms the rock surface location using various contact sensors on the turret and then positions the DRT at a safe stand-off distance (not in contact with the rock). The DRT motor is then energized such that the bristles spin at relatively high speed and the RA then moves the DRT toward the rock surface to a position where the bristles are theoretically engaged. The DRT engagement position and angle may be off by as much as 10 mm and 15°, respectively, in any direction due to RA positioning error. The DRT motor current and encoder are monitored for a stall condition, but otherwise it is an open loop operation where the DRT motor is left energized for a period of time

(~60 seconds) to sweep the rock. The RA then pulls the DRT back away from the rock while the bristles are spinning at low speed so as not to inadvertently foul the cleared area with a sudden stop and dragging of the bristles (an undesirable effect observed during testing). The DRT motor is then de-energized while in free-space.

In addition to the single actuator and RA operational constraints, the other major constraints included the allowable volume and mass for the DRT and the fact that the DRT had to employ a particular JPL-supplied motor model. The DRT was to fit in a cylindrical envelope approximately 134-mm long and 141 mm in diameter. The allowable mass was 950 grams which included the mass of the motor (350 grams). The DRT design was to assume that the motor could provide 28 mN-m of torque at 10,000 rpm.

The DRT engineering challenge could then be boiled down to designing a set of brushes with the reach and compliance to meet the primary functional requirement (i.e., sweep a 45-mm diameter) across the range of surface topography and texture scenarios while not exceeding the tool volume, mass and motor limits. The resulting DRT fit within a cylindrical envelope 154-mm long and 102 mm in diameter and weighed 925 grams. The mechanism is comprised of a JPL-supplied motor integrated with a Honeybee custom-designed planetary gearbox which drove a sub-assembly called the brush block. The brush block consists of an asymmetric set of brushes each on spring loaded pivot (hinge) in order to accommodate the wide variation in surface geometry. A resistive strip heater is bonded to the outside of the planetary gearbox. A rotating post at the center of the brush block guards against overloading the tool's brushes against the rock.

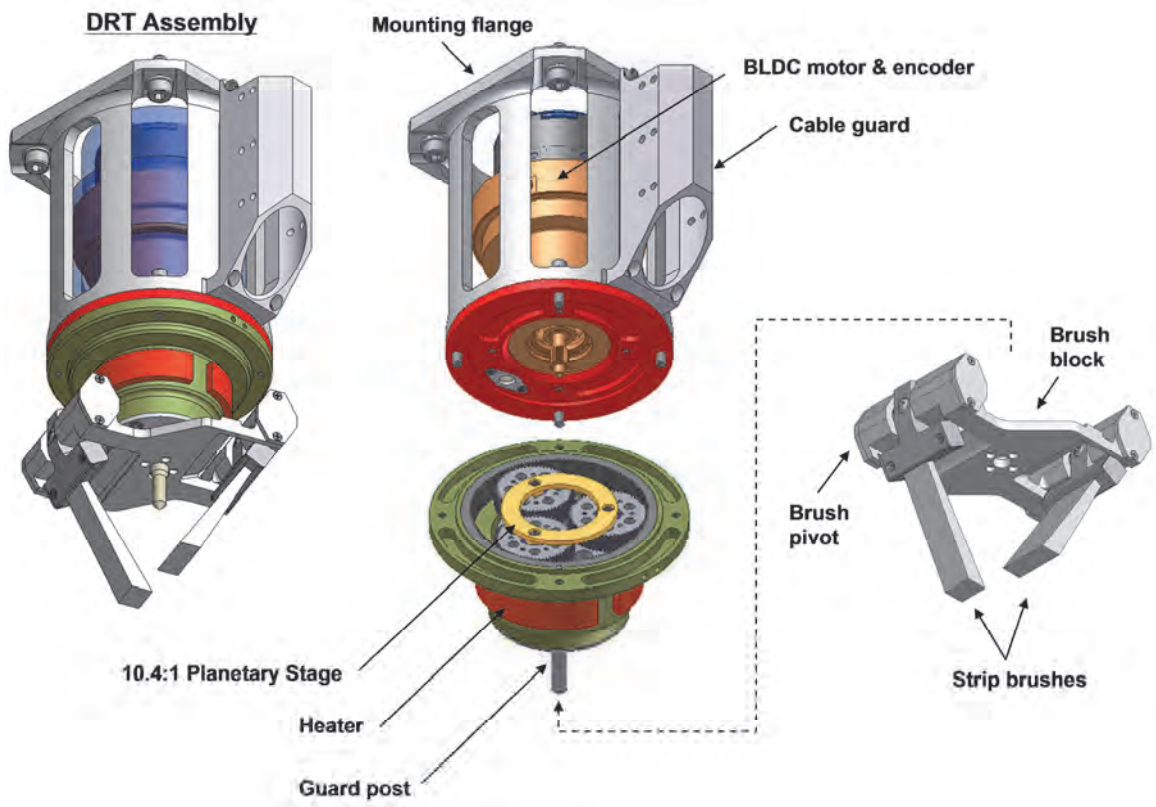

Figure 4. Dust Removal Tool

Brush Block Subassembly

The brush design process was heavily informed by a prototype testing program that lasted beyond the Critical Design Review. Rocks and dust analogs were supplied to Honeybee by JPL. A test and measurement methodology was established which quantitatively assessed brush performance. Per its equipment specification, the DRT dust removal capability was to be demonstrated by clearing 70% of dust particles less than 500 microns by surface area from a natural surface. It was especially important to clear the center of the 45-mm diameter area. Images of the surface were captured via digital camera and analyzed in software to determine the size of the area cleared by the tool. Additionally, the DRT would be required to perform dust removal operations up to 150 times on Mars and therefore a 2x demonstration (300 operations) would need to be performed with the final brush life test model. So quantitative measurements of bristle wear and brush shape degradation were also made to project life.

Initially the team considered several variants of the very simple “brush-on-a-stick” concept (left most image in Figure 5) but soon realized that bristle compliance alone was not enough to compensate for large surface height variations without massive increases in parasitic drag on the motor. Furthermore, relying on bristle compliance also worked the bristles much harder causing wear and flexing that shortened bristle life. So the notion of allowing the brush bristles to pivot about a spring loaded hinge was quickly adopted. The brushes can pivot up to 30° so that large surface height variations (10-20 mm) can be accommodated. By using a soft spring with a flat spring rate to keep the bristles loaded against the rock surface, the bristle contact force and resulting motor torque changes very little.

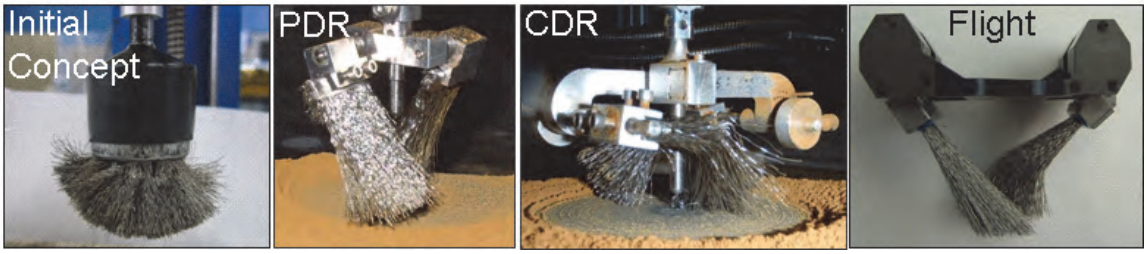

Figure 5. Brush design evolution

		Requirements and Restrictions						
		45 mm Diameter Circle	> 70% Clean	Center Clearing	Avoid Bristle Entanglement	Volume Envelope Restrictions	< 50 N Reaction Load into Turret	< 5 Micron Dust
Brush Geometry	Brush Width	■				■		
	Brush Length					■		
	Wire Bend		■		■			■
Brush Holder Geometry	Brush Offset Distance from Center			■	■			
	Brush Separation Distance			■	■			
	Brush Symmetry	■			■			
	Brush Pivot Axis Distance from Center					■		
	Brush Angle					■		
	Spring Preload		■				■	■
Software and Placement	Brush Speed		■					
	Approach Algorithm			■			■	
	Retract Algorithm	■	■					
	Engagement Distance		■					■
	Brush Duration		■					■

Figure 6. Matrix showing the major brush related design/ performance drivers

Many parameters were discovered to have an effect on the performance of this dual pivoting brush design. These parameters and their relationship to design/performance requirements are illustrated in Figure 6. Following is a summary of findings associated with key brush parameters:

- **Brush offset distance from center** – A large offset distance made it difficult or impossible to clear the center of the 45-mm diameter area; a small offset increased the chances of bristle entanglement around the center post or with bristles from the other brush.
- **Brush separation distance** – Naturally if the brushes were too close they became entangled; a minimum separation distance (~8 mm) was established which yielded best performance (minimal entanglement).
- **Brush symmetry** – It was found that with a symmetric brush design, it was impossible to clear the center of the 45-mm diameter area without severe bristle entanglement; an asymmetric brush design was adopted where one brush (Inner Brush) overlaps and clears the center and most of the area while the other (Outer Brush) assists with clearing the outer part of the area.
- **Engagement distance (brush angle)** – The engagement distance is the distance between the DRT and the rock surface as measured from the tip of the center post to the rock surface; being too close (<10 mm, shallow brush angle) resulted in a poorly cleaned surface while being further away (>10 mm, steep brush angle) resulted in better clearing and better ability of the bristles to pluck dust out of vesicular pits and crevices.
- **Brush width** – There seemed to be a critical brush width (~15 mm or $^1/_3$ the required cleared area diameter) where thinner brushes produced very clear surfaces of smaller diameter and wider brushes produced less clear surface of larger diameter.
- **Wire bend** – Straight bristles had a very difficult time removing fine particles from voids and crevices unless the engagement distance was large enough; forming a bend in the bristles enhanced their ability to “scrub” the surface even at shallow brush angles (close engagement).
- **Brush speed** – Speeds less than 300 rpm did not impart enough energy to effectively remove particles, instead the brushes just pushed the particles around in a circle; at speeds greater than 300 rpm, the brushes are much more effective at clearing the particles – a big difference between 300 rpm and 500 rpm was observed while a negligible difference between 500 rpm and 1000 rpm was observed.
- **Approach algorithm** – Not spinning the brush block while approaching the rock occasionally produced large reaction forces and at times no “center clearing”; spinning while approaching rock reduced axial force on DRT, resulted in symmetric pivoting of brushes and helped to clear the center of the 45-mm diameter area.
- **Retract algorithm** – Spinning at high speeds (or not spinning at all) while retracting tends to pull dust and debris back into cleared area; spinning at lower speeds (100 rpm or less) tends not to drag or eject material into clean areas.

Ultimately, all of the prototype testing resulted in the final flight brush design shown in the far right-hand image in Figure 5. The DRT flight brush bristles were made of a material similar to RAT brush bristles [4]. A brush manufacturer delivered straight brushes of a specified width and Honeybee formed the final brush geometry by bending the bristles around mandrels per a template and potting with a suitable flight-grade adhesive. The bristles were then trimmed to length. At two points in the process the bristle wire and brush assemblies underwent ultrasonic cleaning for contamination control (CC) and planetary protection (PP) reasons. Samples were sent to JPL for CC/PP analysis and approved for flight.

The spring-loaded brush pivots (hinges), Figure 7, were designed to keep the brushes lightly loaded against the rock surface across large variations in surface height relative to the DRT. The pivots allow the brushes to rotate 30° from hard-stop to hard-stop. The whole brush block assembly is designed to withstand inadvertent loading by the RA up to 200 N. This is one reason the pivot shaft is supported by bushings as opposed to small ball bearings. Spring-energized Bal Seals protect the bushings against dust ingress. The Bal Seals were match fit with the shaft to reduce the parasitic drag to near zero at standard temperature and pressure – a similar procedure was used with success for the RAT grinding wheel shaft

and Phoenix Icy Soil Acquisition Device cutting bit shaft [4][7]. The shaft is spring-loaded against a hard-stop by dual torsion springs. End cover-plates with integral spring arbors enclose the spring-bushing area. The pivot shaft-bushing-spring system is dry lubricated.

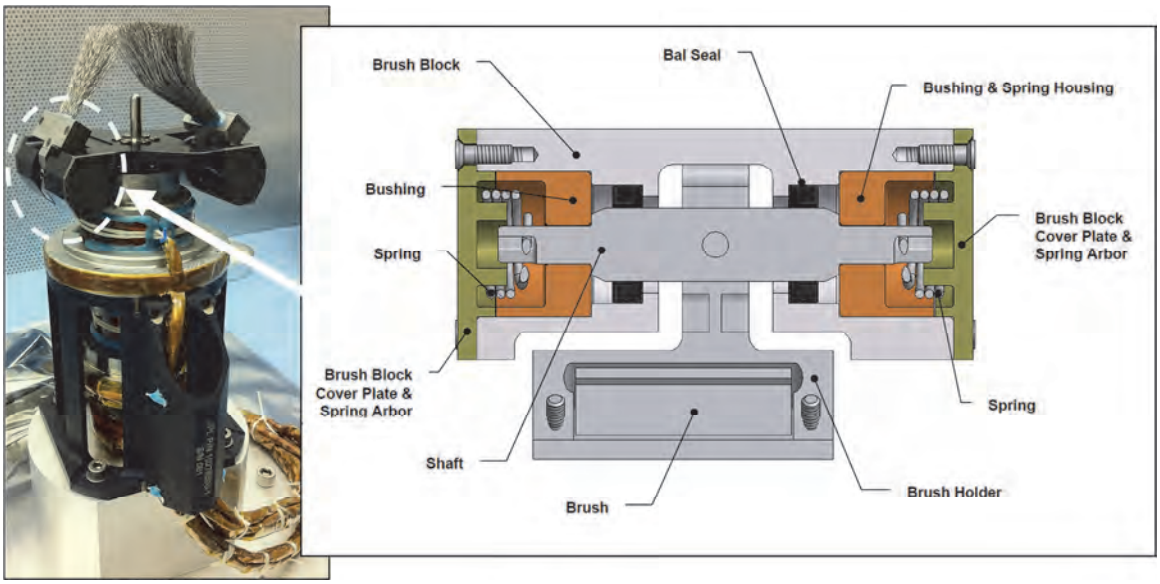

Figure 7. DRT Brush pivot

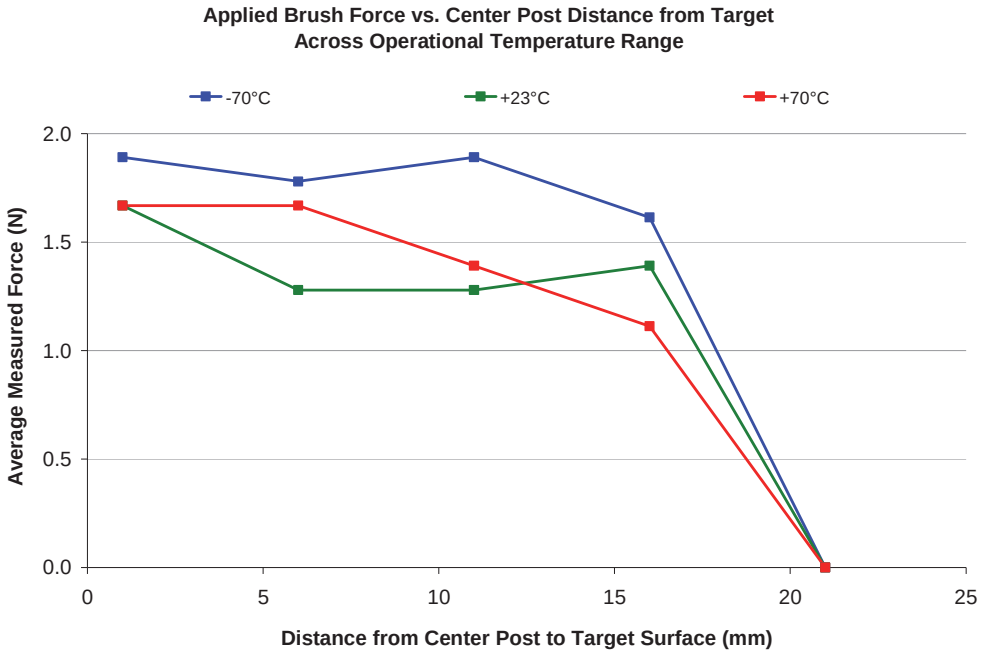

Figure 8. DRT Flight Model brush contact force vs. surface height

Sizing the pivot's springs was an exercise in threading the needle. On the one hand, the springs needed to be strong enough to keep the brushes in contact with the rock over the complete range of pivot motion (including at its relaxed hard stop). And on the other hand they needed to be soft enough such that the brush contact force at the fully compressed pivot position caused very little drag on the motor and the motor torque margin requirement would be met. It only took on the order of 3 N of bristle contact force to achieve the allowable motor current limit. So the springs were designed to deliver about 1.4 N of contact

force at the fully compressed pivot position and the spring rate was selected to be as flat as possible such that the contact force was about 0.4 N at the lower hard-stop.

The brush block subassembly was dynamometer tested across the operational temperature range (-70°C to +70°C). Instead of using a torque watch to directly measure the torque supplied by each pivot axis over the range of motion, a test was designed to measure the net contact force delivered by both brushes against a contact plate instrumented with a load cell. At each temperature set point, the instrumented contact plate was translated toward the DRT brush block as the brush block was spinning at low RPM – this mimicked the flight operational concept. The DRT and contact plate translation stage were configured horizontally such that gravity should not have been a factor. Force measurements were taken at 21 mm (1 mm beyond the brushes reach), 16 mm, 11 mm, 6 mm and 1 mm between the center post tip and the contact plate. Measurements were not taken in the reverse order to quantify friction drag on the pivot axis. The results of this test, shown in Figure 8, were nominal (i.e., the springs produced forces that were within the expected range).

Brush Pivot Problem/Failure Report

Following the dynamometer testing of the DRT Flight Model (FM) and Engineering Model (EM) units and the subsequent delivery of the FM, the DRT EM was performance and life tested across the operational temperature range. During these tests, the EM motor was energized to spin up the brush block while it was positioned above a rock surface in the thermal vacuum chamber. Once at speed, a linear translation stage (ground support equipment playing the part of the RA) moved the DRT to a position of engagement with the rock. After a period on the rock, the motor speed was decreased to a lower setting and the DRT was retracted off the rock. This test procedure was consistent with the manner in which the tool would be used during the mission.

During the -70°C tests, it was observed the EM Inner Brush did not return all the way to its hard-stop following the low speed retraction from the rock. Instead it stopped a few degrees away from the hard-stop. However, the Inner Brush did return to its hard-stop position following the nominal 10-second 900 rpm run. The EM performance and life testing continued until the EM had successfully met its dust removal performance requirements after 2x life (greater than 300 brushing operations).

The Problem Failure Report process was initiated to capture the anomalous Inner Brush behavior and subsequent root cause investigation. The concern was that the pivot (unassisted by centripetal force) was not meeting its torque margin requirement. Per the DRT equipment specification, all actuators were required to demonstrate a minimum margin of 100% on torque required for operation under worst-case conditions where Margin = (Actual/Required – 1)*100%. In this case, the EM Inner Brush pivot spring (the actuator) had apparently failed to supply enough torque to overcome friction and return the brush to its hard-stop. The requirement in this case is that the spring be able to supply twice the torque required to overcome the friction opposing a return to hard stop – this would be considered a margin of 100% or factor of safety (FOS) of 2.

The first thing the team did was to revisit the pivot analytical model used during the design process as well as the as-built in-process test data and dynamometer test data. According to the manufacturing documentation the measured seal drag on the EM's Inner Brush pivot was 50% higher than that of the EM's Outer Brush and both the FM Inner and Outer Brush. This appeared to be the smoking gun. Unfortunately however, the team realized that the dynamometer test approach inadequately demonstrated the torque (or force) margin and it was impossible to draw any further conclusions about the pivot spring's torque margin. Pursuing the seal drag theory, it was hypothesized that seal contraction at cold temperatures had caused the drag torque to spike on the EM Inner Brush seal-shaft combination because it was perhaps past the "knee in the curve" known to exist in these types of configurations. So measurements of seal drag versus diametral interference were made at room temperature using gage pins to create a model (see Figure 9) and the maximum theoretical seal contraction was calculated. According to the model, the EM Inner Brush would have a margin less than 100% (FOS < 2) but the

margin should still be comfortably positive (FOS > 1). It was clear that something was missing from the model.

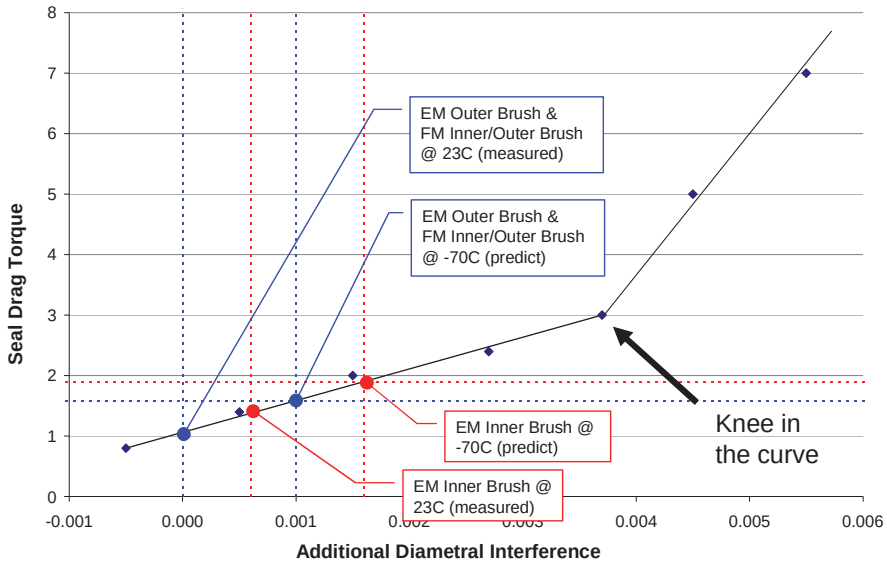

Figure 9. Seal Drag Model

Next a complete disassembly of the EM Inner Brush pivot was performed and documented. Unfortunately, other than very minor evidence of components rubbing (dark marks), there was no clear culprit explaining the problem with the EM Inner Brush pivot. The EM brush block was reassembled and the unit was sent to JPL for further testing.

At JPL, tests were performed at temperature on both the EM and FM to more directly measure the pivot's drag and spring torque and thereby achieve a clear demonstration of torque margin. A general model of the pivot behavior is shown in Figure 10 and assumes drag torque is equal in both directions and of course opposes the direction of motion. So in one direction, the measured torque is the sum of the spring and drag torque. While in the other direction, the measured torque is the difference between the spring and drag torque.

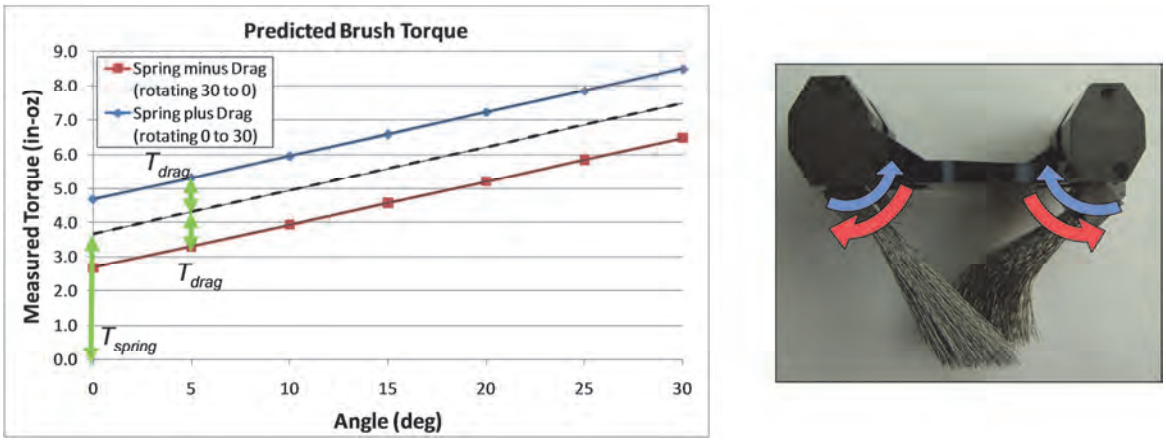

Figure 10. Pivot spring drag torque model

The JPL test results are shown in the columns labeled "0 rpm" in Table 1. At 0 RPM, the brush block pivots demonstrated a margin of 100% or more (FOS ≥ 2) in only one instance for the EM and only one

instance for the FM. In many cases, negative torque margin was calculated. The JPL tests confirmed that the DRT pivot design did not meet the torque margin requirement.

Table 1. DRT Pivot Torque Factor of Safety (FOS) Test Results (min. required FOS: 2.0)

		EM DRT				FM DRT			
Temp (°C)	Test #	Inner Brush		Outer Brush		Inner Brush		Outer Brush	
		0 rpm	900 rpm	0 rpm	900 rpm	0 rpm	900 rpm	0 rpm	900 rpm
+70	Test #1	2.00	6.96	1.24	4.64	1.51	5.59	1.33	4.69
	Test #2	1.78	6.54	1.23	4.60	1.83	6.44	1.56	5.54
+20	Test #1	1.30	5.03	1.58	4.85	1.27	4.79	1.87	4.85
	Test #2	1.23	5.28	1.42	4.63	1.17	4.60	2.20	6.20
-30	Test #1	0.67	3.34	0.61	2.27	0.96	3.61	1.05	3.28
	Test #2	1.06	3.58	0.54	2.29	0.74	3.13	0.52	2.13
-70	Test #1	0.76	2.22	0.47	1.50	0.43	1.87	0.51	1.64
	Test #2	0.57	2.04	0.35	1.33	0.38	1.78	0.64	1.77

Next calculations were repeated to determine the torque margin when taking into account the centripetal forces acting on the brushes when the motor is spinning the brush block at 900 rpm – this was the speed used at the end of each performance test brushing operation after the DRT had been retracted away from the rock. These calculations are shown in the columns labeled “900 rpm” in Table 1. It was determined that operating the DRT at 900 rpm produces a calculated centripetal force that will reliably return the brush pivots to their hard stops. The minimum FOS for the FM in this case is 1.64 (Outer Brush Test #1 at -70°C).

No further work was done to determine root cause and no hardware changes were called for as a flight operations rule that spins the DRT brush block at 900 rpm before each use was deemed an adequate solution by the review board.

Motor & Gearhead Subassembly

A challenge in the DRT design was to overcome the torque margin constraints due to the required use of a predefined motor. Based on the motor performance specifications, torque amplification was necessary and a custom single-stage planetary gearbox was designed (ref. Figure 11). The pinion of the motor was predefined as a long-addendum spur gear. This was likely done to avoid undercutting and increase the load capacity and life of the small pinion, necessitating the use of modified profile planet and ring gears.

Actuator margin analysis (ref. Figure 12) was performed based on those performance parameters as well as thermal limitations provided by JPL based on heat-up analyses. Various parameters were also estimated including seal and bearing losses as well as operational torque. The latter was estimated based on data from brush development tests.

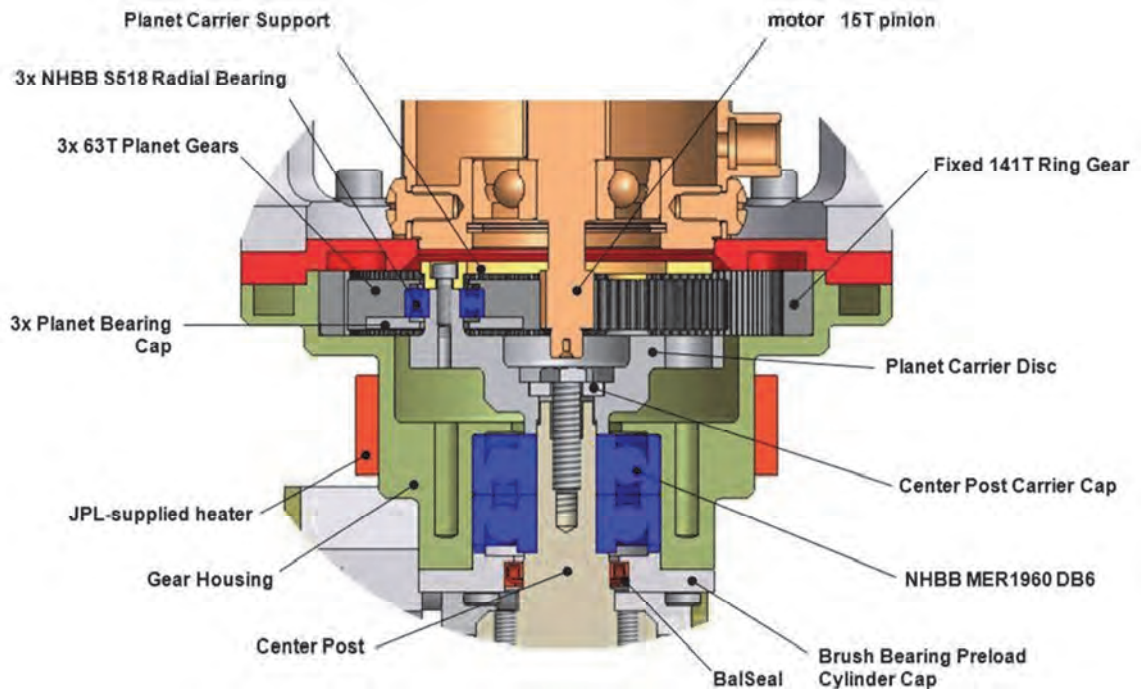

Figure 11. Cross Section of Gearbox Assembly

Analysis predicted that a 10.4:1 reduction ratio gave a torque margin of 140% and a thermal dissipation margin of 475% which exceeded the 125% requirement for a CDR-level design. Reducing the ratio to 6:1 decreases those margins to 41% and 99%, respectively. The gearbox single-stage ratio selection of 10.4:1 is somewhat unconventional when considering planetary gearbox rules of thumb which limit the highest practical reduction ratio to 10:1 due to decreased pinion size and increased sliding within the gear mesh (i.e. decreased efficiency and life).

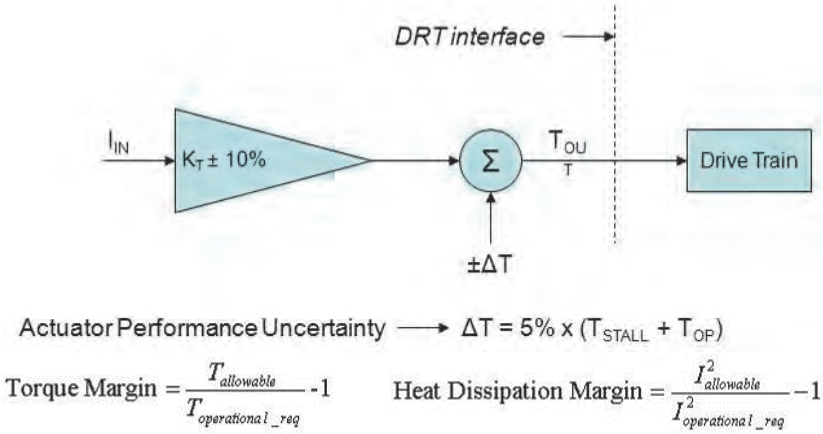

Figure 12. Actuator margin analysis methodology

The specific sliding ratio (SSR) is defined as the sliding velocity divided by the rolling velocity at the gear mesh. The SSR varies along each gear mesh. A higher SSR means that a gear mesh design has relatively more sliding action compared to a lower SSR and would therefore have increased friction and decreased efficiency and life. Therefore it is desirable to design a reduction stage to minimize the SSR within the constraints of other driving requirements. The rate of change of the SSR along the line of action should also be minimized for similar reasons.

The DRT required a high single-stage ratio in order to maintain torque margin on the motor as previously discussed. This in combination with a pre-defined 15T pinion fixed the gear proportions. Figure 13 shows how the SSR at the sun-planet gear mesh for the 10.4:1 design changes during a single mesh cycle. Looking at the lowest and highest points of single tooth contact (LPSTC and HPSTC respectively), i.e., the critical stress jump points, the SSR does not exceed a magnitude of 1.0. The worst-case SSR value occurs on the dedendum of the planet during recess action with a magnitude greater than 3.0. Because the SSR is less than 1.0 at both the LPSTC and HPSTC, the DRT gear design was deemed acceptable.

Other analyses included gear life analysis based on the American Gear Manufacturers Association (AGMA) standards 2001-D04 and 908-B89, backlash analysis, and momentary overload analysis. Backlash analysis included contributions from manufacturing tolerances as well as the operational thermal range to ensure that backlash existed under worst-case stack-up conditions. This was validated via accurate involute profile simulations. Momentary overload calculations included a combination of AGMA 2001-D04 and finite-element analysis (FEA) depending on the gear material selected.

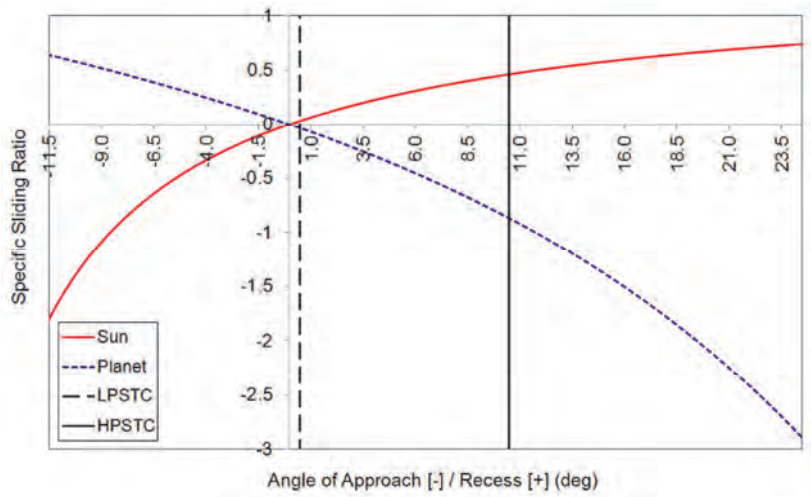

Figure 13. Sun-planet gear mesh specific sliding ratio

To validate the above analyses and verify that the DRT gearbox efficiency was acceptable, the DRT was subjected to output axis dynamometer testing across the operational temperature range. Dynamometer data was acquired at temperature set points (+70°C, +23°C, -55°C, & -70°C) at multiple motor voltages (6, 10, 16 and 22 volts). Speed-torque and current-torque profiles were created. The motor torque constant (K_t) values calculated from the dynamometer data, as shown in Figure 14, match up well with the K_t values measured for the A300 motor prior to integration with the DRT gearbox. This data shows the capability to design efficient planetary gearboxes with relatively high reduction ratios given careful gear tooth profile selection and analysis.

	DRT-integrated A300 Kt values				A300 Kt values	
	6 Volts	10 Volts	16 Volts	22 Volts	16 Volts	21 Volts
Temperature	CCW	CCW	CCW	CCW	CCW	CCW
+70°C	18.0	19.4	20.0	19.2	20.0	20.7
+23°C	18.8	20.4	19.8	20.1	21.1	21.0
-55°C	19.9	20.2	20.5	20.3	N/A	N/A
-70°C	21.4	22.0	20.3	20.7	23.1	23.1

Figure 14. DRT-integrated A300 Kt values across the protoflight thermal range are shown on the left. A300 Kt values (not integrated with DRT are shown on the right.

Lessons Learned

Parasitic Torque Model Shortcomings – The brush pivot drag torque model clearly came up short based on the test results and observations presented above. The lesson learned is to do a more thorough job validating models earlier in the development process (i.e., prior to CDR). The model used in the design process incorporated test data for seal drag from a past program – this data may or may not be valid as it was seal drag for higher operating speeds as opposed to the near static situation measured during the torque margin tests discussed above. One source of drag that may have been overlooked is the friction between the spring and arbor. It is difficult to predict how torsion springs end constraints will behave. Often torsions springs (especially those with few turns and short legs) will cant or cock to one side causing part of the spring to rub against its housing or arbor in an unanticipated manner. This can introduce drag and strange behavior that is difficult to model.

Test Program Inadequacy – In designing a test program that saved time by directly measuring brush contact force over the pivot range of motion, the team overlooked the fact that the test method was not going to collect all the data needed to verify the pivot spring torque margin requirement. Force measurements were taken in only one direction as opposed to both directions which is required to quantify losses due to internal drag. Additionally, while there are benefits to testing in a manner consistent with how the tool would ultimately be used, it was an error to omit a test that isolated the pivot spring and drag torque at temperature. Instead the bristle compliance was included as an unobservable variable in the same test. The lesson learned is to test pivot or hinge torque margin at the pivot/hinge level and to be sure to make a torque measurement in both directions so as to isolate the drag torque from the spring torque.

High-Reduction (10.4:1) Planetary Stage – While not ideal, it was demonstrated that given careful tooth profile selection and analysis, a relatively high-reduction (10.4:1) planetary stage can be an efficient torque amplifier.

Image Processing Provided Easy, Objective Measurement Method – Surface cleanliness can be a very subjective quality that is hard to define. Using image processing algorithms to measure cleanliness and brush performance turned out to be very easy. Its objectivity and ease allowed personnel to focus on collecting more data rather than fiddle with complicated alternative measurement techniques. This method could be used for other more general purposes like quantifying the amount of wear particulate generated in a mechanism over time.

Conclusion

MSL is scheduled to land at Gale Crater on Mars in August 2012. Using the rover's Dust Removal Tool, Earth-bound scientists will sweep away the blinding dust that eventually coats every object on the Martian surface. Spectrometers and cameras will take aim at these freshly exposed surfaces and will gather information that will allow scientists to decide whether those rocks may harbor evidence of organic materials or not. The DRT promises to be as instrumental to MSL's success as the RAT was and is still to the success for MER.

The DRT development process had many challenges. From engineering a brush design that utilizes a single actuator and can deal with 20-mm surface height variations to determining proper methods for testing such a novel device, there were many things learned over the course of the project.

There was a significant discrepancy between a key mechanism analytical model and the tested performance of that mechanism. The root cause of this large discrepancy has not been identified yet. But important lessons were drawn from the experience. In the future, greater consideration will be given to validating such analytical models earlier in the development process and performing component level verification tests on the flight hardware to isolate key parameters.

Acknowledgements

The DRT team at Honeybee Robotics would like to acknowledge and thank the team of scientists, engineers and managers at NASA JPL that offered their input during the DRT development process. The DRT marks the third time that Honeybee has developed a flight qualified robotic end-effector for a landed Mars mission through close collaboration and teamwork with JPL.

References

1. Bishop, J., et al., 2002, A model for formation of dust, soil, and rock coatings on Mars: Physical and chemical processes on the Martian surface, JOURNAL OF GEOPHYSICAL RESEARCH, VOL. 107, NO. E11, 5097, doi:10.1029/2001JE001581.
2. MSL Science Corner: Alpha Particle X-ray Spectrometer, http://msl-scicorner.jpl.nasa.gov/Instruments/APXS/
3. Rieder, R., et al., 1997, The chemical composition of the Martian soil and rocks returned by the mobile Alpha Proton X-ray Spectrometer: Preliminary results from the X-ray mode, Science, 278: 1771-1774.
4. Myrick, T., et al., 2004, Rock Abrasion Tool, Proceedings of the 37th Aerospace Mechanisms Symposium, NASA Johnson Space Center, May 19-21, 2004
5. Herman, J., Davis, K., 2008, Evaluation of Perflouropolyether Lubricant Lifetime in the High Stress and High Stress-Cycle Regime for Mars Applications, Proceedings of the 39th Aerospace Mechanisms Symposium, NASA Marshall Spaceflight Center, May 7-9, 2008
6. Okon, A., 2010, Mars Science Laboratory Drill, Proceedings of the 40th Aerospace Mechanisms Symposium, NASA Kennedy Space Center, May 12-14, 2010
7. Chu, P., et al., 2008, Icy Soil Acquisition Device for the 2007 Phoenix Mars Lander, Proceedings of the 39th Aerospace Mechanisms Symposium, NASA Marshall Spaceflight Center, May 7-9, 2008